

An electro-chemo-mechanical theory with flexoelectricity: application to ionic conductivity of soft solid electrolytes

Anand Mathew, Yashashree Kulkarni*

Department of Mechanical Engineering, University of Houston, Houston, TX 77204, USA

Abstract

Flexible batteries are gaining momentum in several fields, including wearable medical devices and biomedical sensors, flexible displays, and smartwatches. These energy storage devices are subjected to electro-chemo-mechanical effects. Here, we present a theoretical framework that couples diffusion and electromechanical theory with flexoelectricity. As an example, we investigate the effect of flexoelectricity on the ionic conductivity in soft materials. Our analytical results for a thin film made of a soft material reveal that the ionic conductivity is significantly higher at the nanoscale and decreases exponentially to approach the bulk value with increasing film thickness. Furthermore, we find that flexoelectricity reduces the ionic conductivity dramatically at film thickness smaller than the length scale associated with flexoelectricity. This behavior is attributed to the opposite directions of polarization induced by flexoelectricity and the flow of ions driven by the chemical potential. These findings shed light on the interplay between flexoelectricity and diffusion which would be paramount in designing miniaturized energy storage devices.

Keywords: Flexoelectricity, Diffusion, Ionic conductivity, Soft Materials, Electromechanical coupling

1. Introduction

In the rapidly evolving world of technology, energy storage devices are playing an increasingly vital role [1, 2]. This is due to the dramatic increase in demand for miniature self-powering devices, flexible dynamic displays, portable electronics, health care, and fitness-tracking devices, among others [3, 4]. The key components of batteries that govern their efficiency as energy storage devices are the electrodes and the electrolyte. Naturally then, there has been tremendous activity in the areas of materials science and mechanics in understanding and improving the mechanical behavior of the electrodes [5, 6, 7, 8, 9, 10] and electrolytes [11, 12, 13, 14]. The electrolyte facilitates the flow of ions between the electrodes and enables the chemical reactions that generate electrical energy, making the battery functional. Ionic conductivity of electrolytes is an essential characteristic as it determines the efficiency and performance of a battery. Conventional Li-ion batteries work by ionic transport between two electrodes through a non-aqueous liquid electrolyte [15, 16]. Although these energy storage devices have high ionic conductivity [17] which leads to rapid charge and discharge rates, they do not support large deformations which is imperative for designing stretchable and flexible batteries. This is where solid-state batteries show extraordinary promise which has led to a surge of interest in stretchable and flexible solid-state batteries with solid electrolytes [18, 19, 20].

Solid-state batteries with solid electrolytes offer significant advantages over traditional Li-ion batteries, despite their lower ionic conductivity. They not only have a higher energy density [21] but also exhibit superior thermal stability [22], making them an ideal choice for miniature wearable technologies. In addition, solid-state batteries are a safer alternative to Li-ion batteries, as they eliminate the risk of organic solvent leakage [23], which could be toxic. Solid electrolytes also inhibit the growth of lithium dendrites [24],

*Corresponding author

Email address: ykulkarni@uh.edu (Yashashree Kulkarni)

enhancing their overall safety and performance. Particularly in the context of stretchable and flexible batteries, electrolytes that are solid-state as well as soft are ideal candidates. Interestingly, in soft solid electrolytes, the strain gradients resulting from bending and twisting induce a flexoelectric effect, which is further compounded by the presence of ionic diffusion. This interaction between strain gradients and ionic diffusion highlights the importance of studying the coupling of these two effects in soft or flexible solid-state batteries. We refer the reader to a perspective article by Ardebili on the mechanics issues in soft solid electrolytes [25].

Flexoelectricity is the phenomenon that arises due to the coupling between strain gradient and polarization. Unlike piezoelectricity which is another form of electromechanical coupling between uniform strain and polarization that only exists in noncentrosymmetric crystals, flexoelectricity in principle exists in all dielectric/insulating materials [26]. The mathematical expression for polarization due to piezoelectricity and flexoelectricity is given by [27]

$$P_i = d_{ijk}\varepsilon_{jk} + f_{ijkl}\frac{\partial\varepsilon_{jk}}{\partial x_l}. \quad (1)$$

Here, P_i is the component of the polarization vector, ε_{jk} is the component of strain, d_{ijk} and f_{ijkl} are the components of third-order piezoelectric tensor and fourth-order flexoelectric tensor respectively. Flexoelectricity is predominant in soft materials [27, 28, 29], nanomaterials [26] and materials where traditional electromechanical couplings (e.g. piezoelectricity) is absent. Flexoelectricity has been widely studied in the biological context [27, 30, 31, 32, 33, 34, 35] and in liquid crystals [36, 37]. With the advent of soft solid electrolytes for next-generation solid-state batteries, it is critical to understand the mechanics of soft materials subjected to mechanical, chemical, and electrical effects as well as their coupling. To this end, in this paper,

- We formulate a multi-physics theory incorporating diffusion and flexoelectricity for soft materials rooted in the principles of thermodynamics and continuum mechanics. The resulting governing equations enable an understanding of the coupling between the two phenomena.
- By solving a boundary value problem of a soft thin film, we investigate the variation of ionic conductivity as a function of film thickness and stain under the effect of flexoelectricity and diffusion of ions.
- We determine the effect on the overall polarization across the thin film due to the coupling of diffusion with flexoelectricity and provide insights into the interplay between the two effects on the ionic conductivity in the thin film.

The outline of the paper is as follows. In Section 2, we present a comprehensive continuum theory that couples the effect due to flexoelectricity and diffusion. We intend to derive the governing equations and the associated boundary conditions. In Section 3, the governing equations and boundary conditions for the thin film are derived, and the equations are solved numerically. In the subsequent section 4, we analyze and discuss the results to elucidate the significant effects of the coupling of flexoelectricity and diffusion on the behavior of the polymer thin film and its implications for ionic conductivity. In section 5, we conclude by summarizing the key results of the paper and discussing avenues for future studies.

2. A nonlinear continuum theory for electromechanical coupling and diffusion

In this section, we develop a theoretical framework for electro-elastic-diffusive solids incorporating flexoelectricity. Specifically, we present a nonlinear continuum theory for flexoelectricity coupled with diffusion. A theoretical framework for modeling electro-elastic-diffusive systems without considering the effect of flexoelectricity was proposed by Mozaffari et al. [38]. A continuum theory of flexoelectricity was developed by Deng et al. [39]. We will closely follow these two works in formulating an integrated continuum theory for electromechanical coupling and diffusion in soft materials.

Notations: Uppercase and lowercase denote parameters in the reference and current configuration respectively unless specified otherwise. ∇_y , div , curl , and grad denote differential operators in the current configuration and ∇ , Div , Curl , and Grad denote the differential operators in the reference configuration.

2.1. System definition

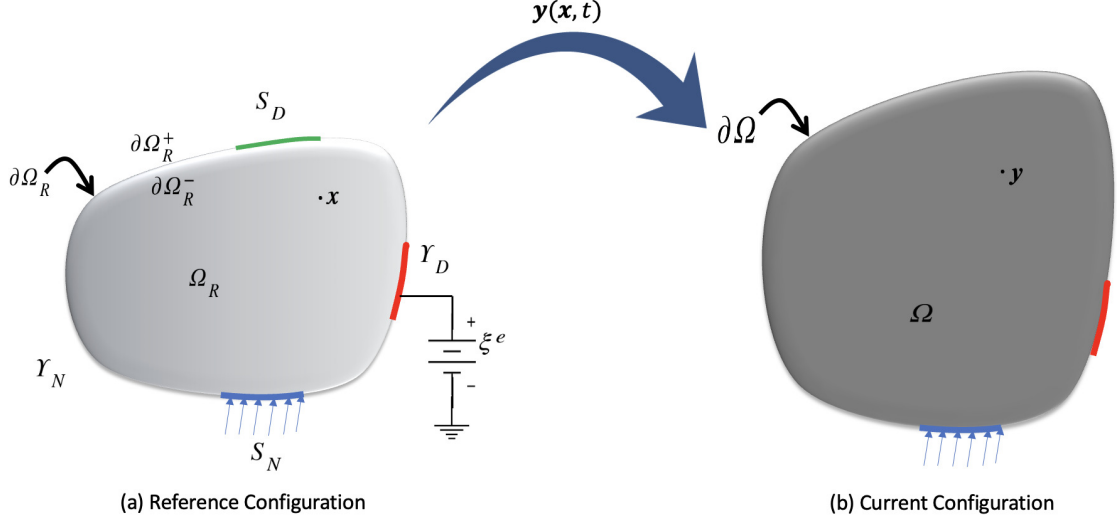


Figure 1: An electro-elastic-diffusive continuum body in (a) reference and (b) current configuration. It is subjected to prescribed displacement on S_D and traction on S_N where $S_N \cup S_D = \partial\Omega_R$ and $S_N \cap S_D = \emptyset$. Υ_D is connected to a solution of ions whereas a flux is applied perpendicular to Υ_N where, $\Upsilon_N \cup \Upsilon_D = \partial\Omega$ and $\Upsilon_N \cap \Upsilon_D = \emptyset$.

As shown in Fig. 1, we consider a continuum body undergoing elastic deformation coupled with diffusion of ions in the presence of an electric field. The thermodynamic state of the system is then determined by the deformation $\mathbf{y}(\cdot, t) : \Omega_R \rightarrow \Omega(t)$, ion volumetric concentration $c(\cdot, t) : \Omega_R \rightarrow \mathbb{R}$ and polarization $\mathbf{P}(\cdot, t) : \Omega_R \rightarrow \mathbb{R}^3$. Here, Ω_R denotes the reference configuration and $\Omega(t)$ denotes the current configuration.

The behavior of the continuum body is consistent with the laws of thermodynamics and Maxwell equations

$$\nabla \times \mathbf{e} = 0, \quad \text{and} \quad \nabla \cdot \mathbf{d} = \rho_f^c, \quad (2)$$

where ρ_f^c is the free charge density, \mathbf{e} is the electric field and \mathbf{d} is the electric displacement in the current configuration. The polarization in the current configuration is given by

$$\mathbf{p} = \mathbf{d} - \epsilon_0 \mathbf{e}. \quad (3)$$

The continuum body interacts with the ambient system through a set of mechanical, chemical, and electrical boundary conditions. The mechanical boundary conditions are imposed on the subdivisions S_D and S_N of $\partial\Omega_R$ as follows:

$$\begin{cases} \mathbf{y}(\mathbf{x}, t) = \mathbf{y}_b(\mathbf{x}, t) & \text{on } S_D, \\ \text{applied external traction} = \mathbf{t}^e(\mathbf{x}, t) & \text{on } S_N, \end{cases} \quad (4)$$

where, $\mathbf{y}_b(\cdot, t) : S_D \rightarrow \mathbb{R}^3$ is the prescribed boundary position in the current configuration. The chemical boundary conditions are imposed on the subdivisions Υ_D and Υ_N of $\partial\Omega_R$ as follows:

$$\begin{cases} \mu = \mu^e(\mathbf{x}, t) & \text{on } \Upsilon_D, \\ \mathbf{J}(\mathbf{x}, t) \cdot \mathbf{n} = J^e & \text{on } \Upsilon_N, \end{cases} \quad (5)$$

where $\mu(\cdot, t) : \Upsilon_D \rightarrow \mathbb{R}$ is the chemical potential, and $\mu^e(\cdot, t)$ is the prescribed chemical potential on Υ_D . $\mathbf{J}(\cdot, t) : \Omega_R \rightarrow \mathbb{R}^3$ is the ionic flux and J^e is the prescribed flux perpendicular to the boundary on Υ_N . As

illustrated in Fig.1, an electric field is applied by an external circuit. The electric field, denoted by $\xi : \Omega_R \rightarrow \mathbb{R}$, has an effect on the transport of ions in the electrolyte. Assuming the boundary potential applied by the external circuit to be ξ^e on Υ_D , we get the electrical boundary condition as follows:

$$\xi = \xi^e(\mathbf{x}) \quad \text{on} \quad \Upsilon_D. \quad (6)$$

2.2. Balance law for species diffusion

The derivation in this section is similar to [40]. Let $c(\mathbf{x}, t)$ be the total number of moles of the diffusing species per unit volume in the reference configuration. The diffusing species can also be characterized by the species flux, $\mathbf{J}(\mathbf{x}, t)$, through the reference outer boundary $\partial\Omega_R^+$. The number of moles of species per unit area per unit time is given by,

$$\int_{\partial\Omega_R^+} J^e = - \int_{\partial\Omega_R^+} \mathbf{J}(\mathbf{x}, t) \cdot \mathbf{n}. \quad (7)$$

The rate of chemical species across the volume, Ω_R , is given by,

$$\int_{\Omega_R} \dot{c} = - \int_{\partial\Omega_R^+} \mathbf{J} \cdot \mathbf{n}. \quad (8)$$

Applying the divergence theorem we get the equation for species mass balance,

$$\int_{\Omega_R} \dot{c} = - \int_{\Omega_R} \text{Div} \mathbf{J}. \quad (9)$$

Since Ω_R is arbitrary, the local form of species balance is given by,

$$\dot{c} + \text{Div} \mathbf{J} = 0 \quad \text{in} \quad \Omega_R. \quad (10)$$

2.3. Rate of external work

The rate of work done on the body has a contribution from mechanical, electrical, and chemical work. This can be expressed as

$$\dot{W} = \dot{W}_{mech} + \dot{W}_{chem} + \dot{W}_{elec}, \quad (11)$$

where the individual terms are given as

$$\dot{W}_{mech} = \int_{\partial\Omega_R^+} \dot{\mathbf{y}} \cdot \mathbf{t}^e, \quad (12)$$

$$\dot{W}_{chem} = - \int_{\partial\Omega_R^+} \mu^e (\mathbf{J} \cdot \mathbf{n}), \quad (13)$$

$$\dot{W}_{elec} = - \int_{\partial\Omega_R^+} q\xi^e (\mathbf{J} \cdot \mathbf{n}) - \int_{\partial\Omega_R^-} \xi (\dot{\mathbf{D}} \cdot \mathbf{n}). \quad (14)$$

Here, \mathbf{D} is the nominal electric displacement which is given by

$$\mathbf{D} = -\epsilon_0 \mathbf{J} \mathbf{C}^{-1} \nabla \xi + \mathbf{F}^{-1} \mathbf{P}, \quad (15)$$

where $\mathbf{F} \equiv \nabla \mathbf{y}$ is the deformation gradient and \mathbf{C} is the right Cauchy-Green deformation tensor. $\partial\Omega_R^+$ is the exterior boundary of $\partial\Omega_R$ and $\partial\Omega_R^-$ is the interior boundary of $\partial\Omega_R$. Thus, Eq. (12) is the rate of work done by the applied traction on the external surface of the continuum body in the reference configuration. The first term in Eq. (13) and Eq. (14) is associated with the chemical flux and electrical flux respectively due to the flow of ions into the continuum body. These terms have a negative sign because the direction of flux and normal are opposite to each other. We note that the electric potential, ξ , may be discontinuous because of the presence of chemical potential. The second term in Eq. (14) can be interpreted considering the body as a capacitor. Thus, consistent with Mozaffari et al. [38], the total rate of work done on the body is

$$\dot{W} = \int_{\partial\Omega_R^+} \dot{\mathbf{y}} \cdot \mathbf{t}^e - \int_{\partial\Omega_R^+} (\mu^e + q\xi^e) (\mathbf{J} \cdot \mathbf{n}) - \int_{\partial\Omega_R^-} \xi (\dot{\mathbf{D}} \cdot \mathbf{n}). \quad (16)$$

110 2.4. Rate of change of free energy

We postulate that the free energy of the body is given by

$$U[\mathbf{y}, c] = U_b[\mathbf{y}, c] + U_{elect}[\mathbf{y}, c], \quad (17)$$

where U_{elect} is the energy associated with the charges whereas U_b includes a contribution to the free energy from deformation, diffusion, and electromechanical coupling. Below, we derive expressions for the rate of change of U_b and U_{elect} .

115 2.4.1. Rate of change of U_b

We postulate that the Helmholtz free energy density, Ψ , defines the constitutive behavior of the body undergoing a quasi-static isothermal process and has the form

$$U_b[\mathbf{y}, c] = \int_{\Omega_R} \Psi(\mathbf{F}, \mathbf{G}, \mathbf{P}, \mathbf{\Pi}, c, \boldsymbol{\kappa}), \quad (18)$$

where \mathbf{G} is the gradient of \mathbf{F} , $\mathbf{\Pi}$ is the gradient of polarization and $\boldsymbol{\kappa}$ is the gradient of concentration. The free energy combines the energy postulated by Deng et al. [39] for flexoelectricity and by Mozaffari et al. [38] for an electro-elastic-diffusive system without flexoelectricity.

From the principle of material frame indifference and from material symmetries, we have,

$$\begin{cases} \Psi(\mathbf{R}\mathbf{F}, \mathbf{R}\mathbf{G}, \mathbf{R}\mathbf{P}, \mathbf{R}\mathbf{\Pi}, c, \mathbf{R}\boldsymbol{\kappa}) = \Psi(\mathbf{F}, \mathbf{G}, \mathbf{P}, \mathbf{\Pi}, c, \boldsymbol{\kappa}) & \forall \mathbf{R} \in SO(3) \\ \Psi(\mathbf{F}\mathbf{Q}, \mathbf{G}\mathbf{Q}, \mathbf{P}\mathbf{Q}, \mathbf{\Pi}\mathbf{Q}, c, \boldsymbol{\kappa}\mathbf{Q}) = \Psi(\mathbf{F}, \mathbf{G}, \mathbf{P}, \mathbf{\Pi}, c, \boldsymbol{\kappa}) & \forall \mathbf{Q} \in \mathcal{G} \end{cases} \quad (19)$$

Here, $SO(3)$ is the set of all rigid rotations and $\mathcal{G} \subset SO(3)$ is the group associated with material symmetries. If a material is isotropic $\mathcal{G} = SO(3)$. Since c is a scalar, and \mathbf{J} is a referential vector field they are both material frame indifferent.

125 Then, the time derivative of Eq. (18) yields

$$\dot{U}_b = \int_{\Omega_R} \frac{d}{dt} \Psi(\mathbf{F}, \mathbf{G}, \mathbf{P}, \mathbf{\Pi}, c, \boldsymbol{\kappa}) \quad (20)$$

$$= \int_{\Omega_R} \frac{\partial \Psi}{\partial \mathbf{F}} \cdot \nabla \dot{\mathbf{y}} + \frac{\partial \Psi}{\partial \mathbf{G}} \cdot \nabla \nabla \dot{\mathbf{y}} + \frac{\partial \Psi}{\partial \mathbf{P}} \cdot \dot{\mathbf{P}} + \frac{\partial \Psi}{\partial \mathbf{\Pi}} \cdot \dot{\mathbf{\Pi}} + \frac{\partial \Psi}{\partial c} \cdot \dot{c} + \frac{\partial \Psi}{\partial \boldsymbol{\kappa}} \cdot \dot{\boldsymbol{\kappa}}. \quad (21)$$

We note that

$$\boldsymbol{\sigma} \equiv \frac{\partial \Psi}{\partial \mathbf{F}} \quad \text{and} \quad \mu \equiv \frac{\partial \Psi}{\partial c}, \quad (22)$$

where $\boldsymbol{\sigma}$ is the local internal Piola-Kirchhoff stress and μ is the chemical potential. We use the balance law for species diffusion to manipulate the last two terms in Eq. (21) and use the divergence theorem to simplify the remaining terms as follows:

$$\begin{aligned} \int_{\Omega_R} \frac{\partial \Psi}{\partial \mathbf{F}} \cdot \nabla \dot{\mathbf{y}} &= \int_{\partial \Omega_R^-} (\boldsymbol{\sigma} \cdot \mathbf{n}) \dot{\mathbf{y}} - \int_{\Omega_R} \text{Div}(\boldsymbol{\sigma}) \cdot \dot{\mathbf{y}}, \\ \int_{\Omega_R} \frac{\partial \Psi}{\partial \mathbf{G}} \cdot \nabla \nabla \dot{\mathbf{y}} &= \int_{\partial \Omega_R^-} \left(\left(\frac{\partial \Psi}{\partial \mathbf{G}} \right) \cdot \mathbf{n} \right) \nabla \dot{\mathbf{y}} - \int_{\partial \Omega_R^-} \left(\text{Div} \left(\frac{\partial \Psi}{\partial \mathbf{G}} \right) \cdot \mathbf{n} \right) \dot{\mathbf{y}} + \int_{\Omega_R} \text{Div} \left(\text{Div} \left(\frac{\partial \Psi}{\partial \mathbf{G}} \right) \right) \cdot \dot{\mathbf{y}}, \\ \int_{\Omega_R} \frac{\partial \Psi}{\partial \mathbf{\Pi}} \cdot \dot{\mathbf{\Pi}} &= \int_{\partial \Omega_R^-} \left(\frac{\partial \Psi}{\partial \mathbf{\Pi}} \cdot \mathbf{n} \right) \dot{\mathbf{P}} - \int_{\Omega_R} \text{Div} \left(\frac{\partial \Psi}{\partial \mathbf{\Pi}} \right) \cdot \dot{\mathbf{P}}, \\ \int_{\Omega_R} \frac{\partial \Psi}{\partial c} \cdot \dot{c} &= - \int_{\Omega_R} \mu (\text{Div} \mathbf{J}) = \int_{\Omega_R} \mathbf{J} \cdot \nabla \mu - \int_{\partial \Omega_R^-} (\mathbf{J} \cdot \mathbf{n}) \mu, \\ \int_{\Omega_R} \frac{\partial \Psi}{\partial \boldsymbol{\kappa}} \cdot \dot{\boldsymbol{\kappa}} &= - \int_{\partial \Omega_R^-} \text{Div} \left(\frac{\partial \Psi}{\partial \boldsymbol{\kappa}} \right) (\mathbf{J} \cdot \mathbf{n}) + \int_{\Omega_R} \mathbf{J} \cdot \text{Grad} \left(\text{Div} \left(\frac{\partial \Psi}{\partial \boldsymbol{\kappa}} \right) \right) + \int_{\partial \Omega_R^-} \left(\frac{\partial \Psi}{\partial \boldsymbol{\kappa}} \cdot \mathbf{n} \right) \text{Div} \mathbf{J}. \end{aligned} \quad (23)$$

The first term of Eq. (23)₂ can be further reduced to

$$\begin{aligned} \int_{\partial\Omega_R^-} \left(\left(\frac{\partial\Psi}{\partial\mathbf{G}} \right) \cdot \mathbf{n} \right) \nabla\dot{\mathbf{y}} &= \int_{\partial\Omega_R^-} \left[\left(\frac{\partial\Psi}{\partial\mathbf{G}} \right) \mathbf{n} \otimes (\mathbf{I} - \mathbf{n} \otimes \mathbf{n}) + \frac{\partial\Psi}{\partial\mathbf{G}} \mathbf{n} \otimes \mathbf{n} \otimes \mathbf{n} \right] \nabla\dot{\mathbf{y}} dA \\ &= \int_{\partial\Omega_R^-} \text{Div} \left(\left(\frac{\partial\Psi}{\partial\mathbf{G}} \right) (\mathbf{n} \otimes (\mathbf{I} - \mathbf{n} \otimes \mathbf{n})) \dot{\mathbf{y}} \right) - \int_{\partial\Omega_R^-} \text{Div} \left(\left(\frac{\partial\Psi}{\partial\mathbf{G}} \right) \mathbf{n} \otimes (\mathbf{I} - \mathbf{n} \otimes \mathbf{n}) \right) \dot{\mathbf{y}} \\ &\quad + \int_{\partial\Omega_R^-} \text{Div} \left(\frac{\partial\Psi}{\partial\mathbf{G}} \right) (\mathbf{n} \otimes \mathbf{n}) (\dot{\mathbf{y}} \cdot \mathbf{n}) . \end{aligned} \quad (24)$$

130 For any vector \mathbf{V} on a closed boundary $\partial\Omega_R^-$, the tangential component of $\nabla\dot{\mathbf{y}}$ is independent of $\dot{\mathbf{y}}$ since [38]

$$\int_{\partial\Omega_R^-} (\text{Div}\mathbf{V}) : (\mathbf{I} - \mathbf{n} \otimes \mathbf{n}) = 0. \quad (25)$$

Then, the first term of the Eq. (24) becomes zero. Denoting $\left(\frac{\partial\Psi}{\partial\mathbf{G}} \right) \mathbf{n} \otimes (\mathbf{I} - \mathbf{n} \otimes \mathbf{n})$ by a tensor $\boldsymbol{\beta}$, we get the rate of change free energy of the body by substituting Eq. (23) and Eq. (24) in Eq. (21) as follows

$$\begin{aligned} \dot{U}_b &= \int_{\partial\Omega_R^-} \text{Div} \left(\frac{\partial\Psi}{\partial\mathbf{G}} \right) (\mathbf{n} \otimes \mathbf{n}) (\dot{\mathbf{y}} \cdot \mathbf{n}) + \int_{\partial\Omega_R^-} \left[\left[\boldsymbol{\sigma} - \text{Div} \left(\frac{\partial\Psi}{\partial\mathbf{G}} \right) \right] \cdot \mathbf{n} - \text{Div}\boldsymbol{\beta} \right] \dot{\mathbf{y}} + \int_{\partial\Omega_R^-} \left(\frac{\partial\Psi}{\partial\boldsymbol{\Pi}} \cdot \mathbf{n} \right) \dot{\mathbf{P}} \\ &\quad + \int_{\Omega_R} \text{Div} \left[\boldsymbol{\sigma} - \text{Div} \left(\frac{\partial\Psi}{\partial\mathbf{G}} \right) \right] \cdot \dot{\mathbf{y}} + \int_{\Omega_R} \left[\frac{\partial\Psi}{\partial\mathbf{P}} - \text{Div} \left(\frac{\partial\Psi}{\partial\boldsymbol{\Pi}} \right) \right] \cdot \dot{\mathbf{P}} + \int_{\Omega_R} \mathbf{J} \cdot \nabla\mu - \int_{\partial\Omega_R^-} (\mathbf{J} \cdot \mathbf{n}) \mu \\ &\quad - \int_{\partial\Omega_R^-} \text{Div} \left(\frac{\partial\Psi}{\partial\boldsymbol{\kappa}} \right) (\mathbf{J} \cdot \mathbf{n}) + \int_{\Omega_R} \mathbf{J} \cdot \text{Grad} \left(\text{Div} \left(\frac{\partial\Psi}{\partial\boldsymbol{\kappa}} \right) \right) + \int_{\partial\Omega_R^-} \left(\frac{\partial\Psi}{\partial\boldsymbol{\kappa}} \cdot \mathbf{n} \right) \text{Div}\mathbf{J}. \end{aligned} \quad (26)$$

2.4.2. Rate of change of U_{elect}

The calculations presented here follow the work of Darbaniyan et al. [41]. The electric energy in the current configuration is given by,

$$U_{elect} = \int_{\Omega} \frac{\epsilon_0}{2} |\nabla_y \xi|^2 dv, \quad (27)$$

where ϵ_0 is the permittivity of free space. Converting Eq. (27) to the reference configuration, we get

$$U_{elect} = \int_{\Omega_R} \frac{\epsilon_0}{2} J |\mathbf{F}^{-T} \nabla \xi|^2 dV, \quad (28)$$

135 where we recall that $\nabla_y \xi = \mathbf{F}^{-T} \nabla \xi$ and $dv = JdV$, J is the Jacobian. Using standard results from continuum mechanics [41],

$$\dot{\mathbf{F}}^{-1} = -\mathbf{F}^{-1} \dot{\mathbf{F}} \mathbf{F}^{-1}, \quad (29)$$

$$\dot{j} = J \mathbf{F}^{-T} \cdot \dot{\mathbf{F}}, \quad (30)$$

$$\overline{\dot{\mathbf{J}} \mathbf{C}^{-1}} = -J \mathbf{F}^{-1} \dot{\mathbf{F}} \mathbf{F}^{-T} - J \mathbf{C}^{-1} \dot{\mathbf{F}}^T \mathbf{F}^{-T} + J (\mathbf{F}^{-T} \cdot \dot{\mathbf{F}}) \mathbf{C}^{-1}, \quad (31)$$

we get

$$\frac{\epsilon_0}{2} \nabla \xi \cdot \overline{\dot{\mathbf{J}} \mathbf{C}^{-1}} \nabla \xi = -\epsilon_0 J \dot{\mathbf{F}} \cdot \left[(\mathbf{F}^{-T} \nabla \xi) \otimes (\mathbf{C}^{-1} \nabla \xi) - \frac{1}{2} |\mathbf{F}^{-T} \nabla \xi|^2 \mathbf{F}^{-T} \right]. \quad (32)$$

140 Taking the time derivative of Eq. (28) and using the divergence theorem, we get,

$$\dot{U}_{elect} = \int_{\Omega_R} \left[\nabla \dot{\mathbf{y}} \cdot \boldsymbol{\Sigma}_{MW} + \nabla \xi \cdot \mathbf{F}^{-1} \dot{\mathbf{P}} + \xi (\nabla \cdot \dot{\mathbf{D}}) \right] - \int_{\partial\Omega_R^-} \xi (\dot{\mathbf{D}} \cdot \mathbf{n}). \quad (33)$$

where Σ_{MW} is the Maxwell stress expressed as

$$\Sigma_{MW}[\mathbf{F}, \mathbf{P}] = (\mathbf{F}^{-T} \nabla \xi) \otimes (\epsilon_0 J \mathbf{C}^{-1} \nabla \xi - \mathbf{F}^{-1} \mathbf{P}) - \frac{\epsilon_0}{2} |\mathbf{F}^{-T} \nabla \xi| \mathbf{F}^{-T}. \quad (34)$$

Using Eq. (15) and the Maxwell equation, $\text{Div} \mathbf{D} = \rho_f$ where ρ_f is the free charge density in the reference configuration, we get

$$\text{Div} \mathbf{D} = q(c - c_0(\mathbf{x})), \quad (35)$$

where, c_0 is the concentration of immobile ions. Taking the time derivative we get,

$$\nabla \cdot \dot{\mathbf{D}} = q\dot{c}. \quad (36)$$

145 Using the Maxwell equation, $\mathbf{J}_e + \dot{\mathbf{D}} = 0$, ignoring magnetic effects, we get,

$$\dot{\mathbf{D}} = -\mathbf{J}_e = -q\mathbf{J}, \quad (37)$$

where \mathbf{J}_e is the electric current density in the reference configuration. Using Eqs. (36)-(37) in Eq. (33) yields

$$\dot{U}_{elect} = \int_{\Omega_R} \left[\nabla \dot{\mathbf{y}} \cdot \Sigma_{MW} + \nabla \xi \cdot \mathbf{F}^{-1} \dot{\mathbf{P}} + q\dot{c}\xi \right] + \int_{\partial\Omega_R^-} q\xi(\mathbf{J} \cdot \mathbf{n}). \quad (38)$$

Applying the divergence theorem to the first and last term, we get

$$\dot{U}_{elect} = \int_{\Omega_R} \left[-\dot{\mathbf{y}} \cdot \text{Div}(\Sigma_{MW}) + (\mathbf{F}^{-T} \cdot \nabla \xi) \dot{\mathbf{P}} + \mathbf{J} \cdot \nabla(q\xi) \right] + \int_{\partial\Omega_R^-} \dot{\mathbf{y}} (\Sigma_{MW} \cdot \mathbf{n}). \quad (39)$$

2.5. Rate of Energy Dissipation

The rate of energy dissipation is given by,

$$\dot{D} = \dot{W} - \dot{U}_b - \dot{U}_{elect}. \quad (40)$$

Substituting Eqs. (16), (26), and (39) in Eq. (40), we get the expression for the rate of energy dissipation as

$$\begin{aligned} \dot{D} = & \int_{\Omega_R} \text{Div} \left[\boldsymbol{\sigma} - \text{Div} \left(\frac{\partial \Psi}{\partial \mathbf{G}} \right) + \Sigma_{MW} \right] \cdot \dot{\mathbf{y}} - \int_{\Omega_R} \mathbf{J} \cdot \nabla(q\xi + \mu) - \int_{\Omega_R} \left[\frac{\partial \Psi}{\partial \mathbf{P}} - \text{Div} \left(\frac{\partial \Psi}{\partial \mathbf{\Pi}} \right) + \mathbf{F}^{-T} \cdot \nabla \xi \right] \cdot \dot{\mathbf{P}} \\ & - \int_{\partial\Omega_R^+} (\mu^e + q\xi^e)(\mathbf{J} \cdot \mathbf{n}) + \int_{\partial\Omega_R^-} (\mu + q\xi)(\mathbf{J} \cdot \mathbf{n}) + \int_{\partial\Omega_R^+} \dot{\mathbf{y}} \cdot \mathbf{t}^e - \int_{\partial\Omega_R^-} \left(\frac{\partial \Psi}{\partial \mathbf{\Pi}} \cdot \mathbf{n} \right) \dot{\mathbf{P}} \\ & + \int_{\partial\Omega_R^-} \text{Div} \left(\frac{\partial \Psi}{\partial \boldsymbol{\kappa}} \right) (\mathbf{J} \cdot \mathbf{n}) - \int_{\Omega_R} \mathbf{J} \cdot \text{Grad} \left(\text{Div} \left(\frac{\partial \Psi}{\partial \boldsymbol{\kappa}} \right) \right) - \int_{\partial\Omega_R^-} \left(\frac{\partial \Psi}{\partial \boldsymbol{\kappa}} \cdot \mathbf{n} \right) \text{Div} \mathbf{J} \\ & - \int_{\partial\Omega_R^-} \left[\left(\boldsymbol{\sigma} - \text{Div} \left(\frac{\partial \Psi}{\partial \mathbf{G}} \right) + \Sigma_{MW} \right) \cdot \mathbf{n} - \text{Div} \boldsymbol{\beta} \right] \cdot \dot{\mathbf{y}} - \int_{\partial\Omega_R^-} \left(\frac{\partial \Psi}{\partial \mathbf{G}} \right) (\mathbf{n} \otimes \mathbf{n}) (\dot{\mathbf{y}} \cdot \mathbf{n}). \quad (41) \end{aligned}$$

150 2.6. Governing Equations and Boundary Conditions

According to the second law of thermodynamics, $\dot{\mathbf{D}} \geq 0$ for all isothermal processes. We follow the Coleman-Noll procedure to ensure that the laws of thermodynamics are satisfied and obtain the following

$$\begin{cases} -\mathbf{J} \cdot \nabla \left(q\xi + \mu + \text{Div} \left(\frac{\partial \Psi}{\partial \boldsymbol{\kappa}} \right) \right) \geq 0 & \text{in } \Omega_R, \\ \text{Div} \left[\boldsymbol{\sigma} - \text{Div} \left(\frac{\partial \Psi}{\partial \mathbf{G}} \right) + \Sigma_{MW} \right] = 0 & \text{in } \Omega_R, \\ \left[\frac{\partial \Psi}{\partial \mathbf{P}} - \text{Div} \left(\frac{\partial \Psi}{\partial \mathbf{\Pi}} \right) + \mathbf{F}^{-T} \cdot \nabla \xi \right] = 0 & \text{in } \Omega_R, \\ \text{Div} \mathbf{D} = \rho_f & \text{in } \Omega_R. \end{cases} \quad (42)$$

We note that Eq. (42)₂ is the mechanical equilibrium equation accounting for electromechanical coupling. Eq. (42)₃ yields an additional equation required to solve for polarization. Eq. (42)₄ is the Maxwell equation. The inequality in Eq. (42)₁ can be satisfied by assuming the constitutive relation for diffusion to be of the form

$$\mathbf{J} = c\mathbf{v}, \quad \mathbf{v} = -\gamma(\mathbf{x})\nabla \left(q\xi + \mu + \text{Div} \left(\frac{\partial\Psi}{\partial\boldsymbol{\kappa}} \right) \right), \quad (43)$$

where \mathbf{v} is the linear mobility. Thus, Eq. (42)₁ recovers the diffusion equation for ion concentration, c . To summarize, the electro-mechanical-diffusive system should satisfy the following governing equations

$$\begin{cases} \dot{c} + \text{Div}\mathbf{J} = 0 & \mathbf{J} = -c\gamma(\mathbf{x})\nabla \left(q\xi + \mu + \text{Div} \left(\frac{\partial\Psi}{\partial\boldsymbol{\kappa}} \right) \right) & \text{in } \Omega_R, \\ \text{Div} \left[\boldsymbol{\sigma} - \text{Div} \left(\frac{\partial\Psi}{\partial\mathbf{G}} \right) + \boldsymbol{\Sigma}_{MW} \right] = 0 & & \text{in } \Omega_R, \\ \left[\frac{\partial\Psi}{\partial\mathbf{P}} - \text{Div} \left(\frac{\partial\Psi}{\partial\boldsymbol{\Pi}} \right) + \mathbf{F}^{-T} \cdot \nabla\xi \right] = 0 & & \text{in } \Omega_R, \\ \text{Div}\mathbf{D} = \rho_f & & \text{in } \Omega_R, \end{cases} \quad (44)$$

and boundary conditions

$$\begin{cases} \left(\boldsymbol{\sigma} - \text{Div} \left(\frac{\partial\Psi}{\partial\mathbf{G}} \right) + \boldsymbol{\Sigma}_{MW} \right) \cdot \mathbf{n} - \mathbf{t}^e - \text{Div}\boldsymbol{\beta} = 0 & \text{on } S_N, \\ \frac{\partial\Psi}{\partial\boldsymbol{\Pi}} \cdot \mathbf{n} = 0 & \text{on } \partial\Omega_R, \\ \mu^e + q\xi^e = \mu + q\xi + \text{Div} \left(\frac{\partial\Psi}{\partial\boldsymbol{\kappa}} \right) & \text{on } \Upsilon_D, \\ \mathbf{J} \cdot \mathbf{n} = 0 & \text{on } \partial\Omega_R \setminus \Upsilon_D, \\ \frac{\partial\Psi}{\partial\boldsymbol{\kappa}} \cdot \mathbf{n} = 0 & \text{on } \partial\Omega_R, \\ \frac{\partial\Psi}{\partial\mathbf{G}} \mathbf{n} \otimes \mathbf{n} = 0 & \text{on } \partial\Omega_R. \end{cases} \quad (45)$$

3. Example of an electro-elastic-diffusive system - a soft solid electrolyte

The boundary value problem derived in Eq. (44) and Eq. (45) represents a general three-dimensional nonlinear continuum theory incorporating diffusion and electromechanical coupling with flexoelectricity. To demonstrate the coupled behavior of an electro-elastic-diffusive system, we consider a simple one-dimensional soft solid electrolyte as shown in Fig. 2. Our aim is to gain insights into the coupling between diffusion and electromechanical coupling. Specifically, we wish to elucidate the effect of flexoelectricity and the diffusion of ions on polarization and study their interplay in determining the ionic conductivity of electrolytes. Since electrostatics and flexoelectricity induce characteristic length scales into the problem, we will also investigate how ionic conductivity varies as a function of the film thickness.

3.1. Governing equations

To this end, consider a thin film made of polyvinylidene fluoride (PVDF) with film thickness, w . For a linearized theory, we expand the Helmholtz free energy density Ψ up to quadratic terms to obtain,

$$\begin{aligned} \Psi(\mathbf{F}, \mathbf{G}, \mathbf{P}, \boldsymbol{\Pi}, c; \mathbf{x}) = & \alpha_{el}(\mathbf{x})\text{Tr}(\mathbf{F} - \mathbf{I}) + \frac{\beta(\mathbf{x})}{2}(c - c_0(\mathbf{x}))^2 + \hat{\mu}(\mathbf{x})(c - c_0(\mathbf{x})) + \frac{1}{2}\mathbf{P} \cdot \mathbf{a}(\mathbf{x})\mathbf{P} \\ & + \frac{1}{2}(\mathbf{F} - \mathbf{I}) : \mathbb{C}(\mathbf{x})(\mathbf{F} - \mathbf{I}) + \mathbf{P} \cdot \mathbf{f}(\mathbf{x})\mathbf{G} + \frac{1}{2}\boldsymbol{\Pi} : \mathbf{b}(\mathbf{x})\boldsymbol{\Pi} + \boldsymbol{\Pi} : \mathbf{e}(\mathbf{x})(\mathbf{F} - \mathbf{I}). \end{aligned} \quad (46)$$

170 Here, \mathbf{I} is the identity matrix, $\hat{\mu}(\mathbf{x})$ is the standard chemical potential or the chemical potential of the pure ion, $\alpha_{el}(\mathbf{x})$ is the coupling coefficient for elasto-diffusion, $\beta(\mathbf{x})$ is the chemistry modulus, $\mathbf{a}(\mathbf{x})$ is the reciprocal dielectric susceptibility, $\mathbb{C}(\mathbf{x})$ is the fourth-order elasticity tensor satisfying major and minor symmetries ($\mathbb{C}_{ijkl} = \mathbb{C}_{klij} = \mathbb{C}_{ijlk}$), $\mathbf{f}(\mathbf{x})$ is the fourth order flexoelectric tensor, $\mathbf{b}(\mathbf{x})$ is the polarization gradient-polarization gradient coupling tensor, $\mathbf{e}(\mathbf{x})$ is the coupling tensor corresponding to polarization gradient and strain proposed by Mindlin [42]. For the sake of simplicity, we have ignored the contribution
175 from the concentration gradient, $\boldsymbol{\kappa}$ to the free energy. Finally, we note that the material properties are explicitly specified to be functions of \mathbf{x} . For brevity, in the subsequent calculations, this dependence on \mathbf{x} will be tacitly assumed.

In our boundary value problem, we consider a classical electro-diffusion model known as the Poisson-Boltzmann-Nernst-Planck (PBNP) model [43, 38]. Consistent with this model, we introduce the electro-chemical potential and the Deybe length defined respectively as

$$\phi = \mu + q\xi \quad \text{and} \quad \lambda = \sqrt{\frac{\epsilon_0\beta}{q^2}}, \quad (47)$$

where q is the charge of the diffusing particle. From Eq. (22)₂ we get the relation

$$\mu = \alpha_{el}\nabla \cdot \mathbf{u} + \beta(c - c_0) + \hat{\mu}, \quad (48)$$

which yields

$$c - c_0 = \frac{1}{\beta}(\mu - \hat{\mu} - \alpha_{el}\nabla \cdot \mathbf{u}). \quad (49)$$

Using Eq. (47) and Eq. (49) the governing equations now take the form,

$$\begin{cases} \dot{c} + \text{Div}(-c\gamma\nabla\phi) = 0 & \text{in } \Omega_R, \\ \text{Div} \left[\frac{\partial\Psi}{\partial\mathbf{F}} - \text{Div} \left(\frac{\partial\Psi}{\partial\mathbf{G}} \right) + \boldsymbol{\Sigma}_{MW} \right] = 0 & \text{in } \Omega_R, \\ \left[\frac{\partial\Psi}{\partial\mathbf{P}} - \text{Div} \left(\frac{\partial\Psi}{\partial\mathbf{H}} \right) + \mathbf{F}^{-T} \cdot \nabla\xi \right] = 0 & \text{in } \Omega_R, \\ \text{Div}(-J\mathbf{C}^{-1}\nabla\xi + \frac{1}{\epsilon_0}\mathbf{F}^{-1}\mathbf{P}) + \frac{\xi}{\lambda^2} = \frac{q}{\epsilon_0\beta}(\phi - \hat{\mu} - \alpha_{el}\nabla \cdot \mathbf{u}) & \text{in } \Omega_R. \end{cases} \quad (50)$$

185 Assuming small strain with $|\nabla\mathbf{u}| \ll 1$, Eqs. (50) can be further simplified. The Maxwell stress also vanishes under small deformation assumption [39, 38]. This yields

$$\begin{cases} \dot{c} + \text{Div}(-c\gamma\nabla\phi) = 0 & \text{in } \Omega_R, \\ \text{Div} \left[\frac{\partial\Psi}{\partial\mathbf{F}} - \text{Div} \left(\frac{\partial\Psi}{\partial\mathbf{G}} \right) \right] = 0 & \text{in } \Omega_R, \\ \left[\frac{\partial\Psi}{\partial\mathbf{P}} - \text{Div} \left(\frac{\partial\Psi}{\partial\mathbf{H}} \right) + \nabla\xi \right] = 0 & \text{in } \Omega_R, \\ \text{Div}(-\nabla\xi + \frac{1}{\epsilon_0}\mathbf{P}) + \frac{\xi}{\lambda^2} = \frac{q}{\epsilon_0\beta}(\phi - \hat{\mu} - \alpha_{el}\nabla \cdot \mathbf{u}) & \text{in } \Omega_R. \end{cases} \quad (51)$$

For a thin film, we assume that the fields only vary in the thickness direction. Let the direction perpendicular to the film be x_1 as shown in Figure 2. Substituting the one-dimensional Helmholtz free energy density, Eq. 46, in Eqs. (51), we arrive at the following simplified governing equations,

$$\begin{cases} \dot{c} + \frac{d}{dx_1}(-c\gamma\nabla\phi) = 0 & \text{in } \Omega_R, \\ \left(\mathbb{C} - \frac{\alpha_{el}^2}{\beta} \right) \frac{d^2u}{dx_1^2} + h \frac{d^2P}{dx_1^2} + \frac{\alpha_{el}}{\beta} \frac{d\mu}{dx_1} = 0 & \text{in } \Omega_R, \\ h \frac{d^2u}{dx_1^2} + b \frac{d^2P}{dx_1^2} - aP - \frac{d\xi}{dx_1} = 0 & \text{in } \Omega_R, \\ \frac{d}{dx_1} \left(-\frac{d\xi}{dx_1} \right) + \frac{1}{\epsilon_0} \frac{dP}{dx_1} + \frac{\xi}{\lambda^2} = \frac{q}{\epsilon_0\beta} \left(\phi - \hat{\mu} - \alpha_{el} \frac{du}{dx_1} \right) & \text{in } \Omega_R. \end{cases} \quad (52)$$

190 Here, $h = e - f$. Finally, assuming open circuit conditions i.e. $\phi = 0$ the governing equations take the form

$$\begin{cases} \dot{c} = 0 \quad J = -c\gamma\nabla\phi & \text{in } \Omega_R, \\ \left(\mathbb{C} - \frac{\alpha_{el}^2}{\beta} \right) \frac{d^2u}{dx_1^2} + h \frac{d^2P}{dx_1^2} + \frac{\alpha_{el}}{\beta} \frac{d\mu}{dx_1} = 0 & \text{in } \Omega_R, \\ h \frac{d^2u}{dx_1^2} + b \frac{d^2P}{dx_1^2} - aP + \frac{1}{q} \frac{d\mu}{dx_1} = 0 & \text{in } \Omega_R, \\ \frac{d^2\mu}{dx_1^2} + \frac{q}{\epsilon_0} \frac{dP}{dx_1} - \frac{\mu}{\lambda^2} = -\frac{1}{\lambda^2} \left(\hat{\mu} + \alpha_{el} \frac{du}{dx_1} \right) & \text{in } \Omega_R. \end{cases} \quad (53)$$

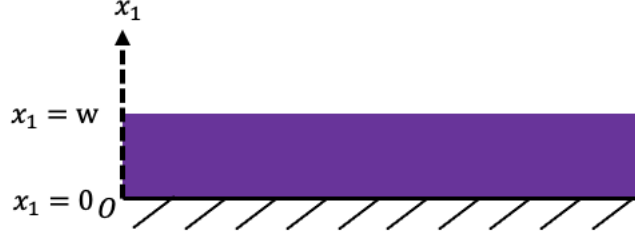


Figure 2: Schematic of a polymer thin film of thickness w in the x_1 direction. The film is held fixed at $x_1 = 0$. This simplifies the boundary value problem to a 1-D problem.

3.2. Boundary conditions

We apply the following boundary conditions:

1. Assuming $\bar{\varepsilon}$ to be the average normal strain in the film, the displacements at the top and bottom of the film are given as

$$u \Big|_{x_1=w} - u \Big|_{x_1=0} = w\bar{\varepsilon}. \quad (54)$$

2. The electric tensor, Λ , is specified to be zero at both ends of the film. The electric tensor, conjugate to the polarization gradient, is defined as

$$\Lambda = \frac{d\Psi}{d\Pi} = e \frac{du}{dx_1} + b \frac{dP}{dx_1}. \quad (55)$$

Hence, the boundary conditions are given by,

$$e \frac{du}{dx_1} \Big|_{x_1=w} + b \frac{dP}{dx_1} \Big|_{x_1=w} = 0. \quad (56)$$

$$e \frac{du}{dx_1} \Big|_{x_1=0} + b \frac{dP}{dx_1} \Big|_{x_1=0} = 0. \quad (57)$$

3. The chemical potential μ and its derivative μ' are prescribed on the boundaries as follows,

$$\mu \Big|_{x_1=0} = \mu_0, \quad (58)$$

$$\mu' \Big|_{x_1=w} - \mu' \Big|_{x_1=0} = qE, \quad (59)$$

where E is the applied electric field.

4. Results and Discussion

In this section, we present our results for the electro-chemo-mechanical behavior of a polymer thin film by solving the boundary value problem derived in the previous section. We chose polyvinylidene fluoride (PVDF) as the material for the thin film. The material properties for PVDF are mentioned in [Appendix B](#). The governing equations in Eq. (53) are solved for the boundary conditions in Eqs. (54)-(59) using the NDSolve package in Mathematica [44] for a fully coupled electromechanical diffusive system. We also solve the boundary value problem for two more cases to facilitate a comparative study of the different effects – electromechanical coupling with diffusion but without flexoelectricity (this reduces to the model proposed by Mozaffari et al. [38]) and electromechanical coupling with flexoelectricity but without diffusion (this reduces to a one-dimensional system based on the theory presented by Deng et al. [39]).

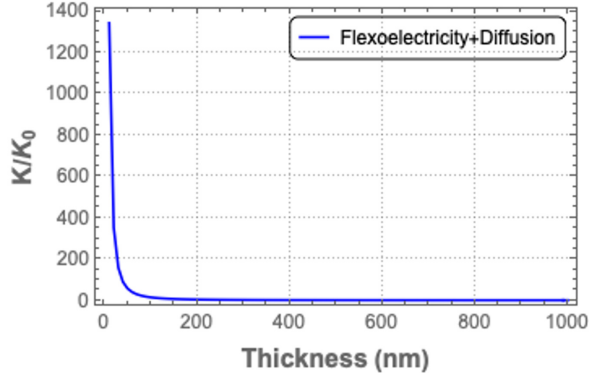


Figure 3: Normalized ionic conductivity for varying thickness for a thin film subjected to 5% strain in an electro-elastic-diffusive system with flexoelectricity. The ionic conductivity is normalized by the conductivity at the initial concentration.

Fig. 3 shows the variation of the normalized ionic conductivity with the film thickness under the effect of flexoelectricity and diffusion at 5% uniaxial strain. The ionic conductivity is calculated based on the solution for concentration $c(x_1)$ using the expression derived by Mozaffari et al. [38]. For convenience, we have summarized the derivation in Appendix A. We observe that the ionic conductivity increases exponentially as the film thickness approaches the Debye length for PVDF which is about 4 nm. The ionic conductivity rapidly approaches the bulk value when the film thickness is greater than 200 nm. We note that the lengthscale introduced by flexoelectricity is on the same order as the radius of gyration which is about 280 nm for PVDF.

To isolate the effect of flexoelectricity on the ionic conductivity we plot the normalized ionic conductivity as a function of strain for a 50 nm and a 100 nm thin film as shown in Fig. 4 and Fig. 5 respectively. We make two observations here. For a 50 nm thin film, the ionic conductivity in the absence of flexoelectricity is almost tenfold higher than in the case with flexoelectricity (Figs. 4(a) and 4(b)). This indicates that for the particular boundary value problem studied here, flexoelectricity appears to reduce the ionic conductivity dramatically. However, for a 100 nm thin film, the ionic conductivity in the absence of flexoelectricity is only slightly greater than in the case with flexoelectricity (Figs. 5(a) and 5(b)). Taken together, Figs. 4 and 5 reveal that flexoelectricity has a much greater impact on ionic conductivity at small film thickness and has no effect when the film thickness is on the order of the flexoelectricity lengthscale and larger.

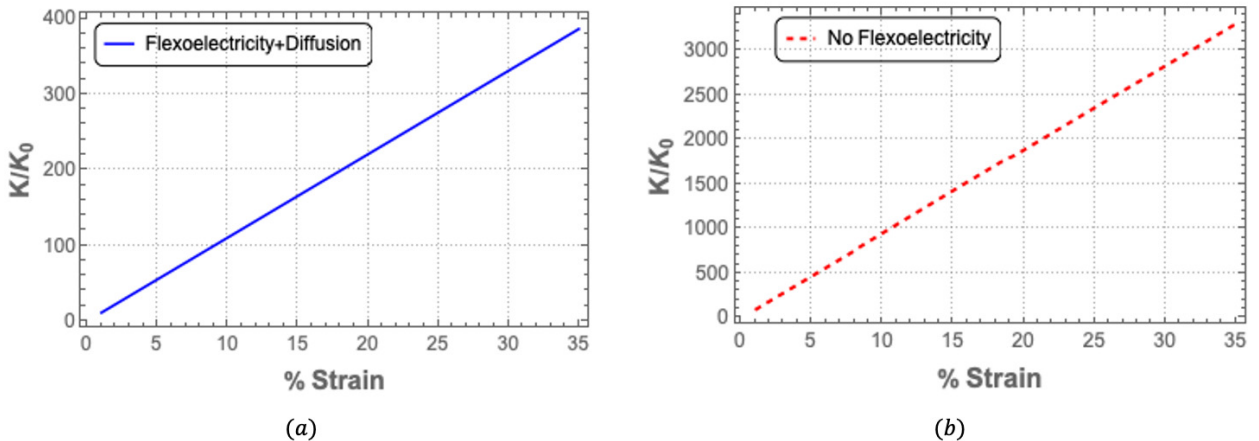


Figure 4: Normalized ionic conductivity of a thin film of thickness 50 nm as a function of uniaxial strain for 4(a) an electro-elastic-diffusive system with flexoelectricity, and 4(b) an electro-diffusive system without flexoelectricity.

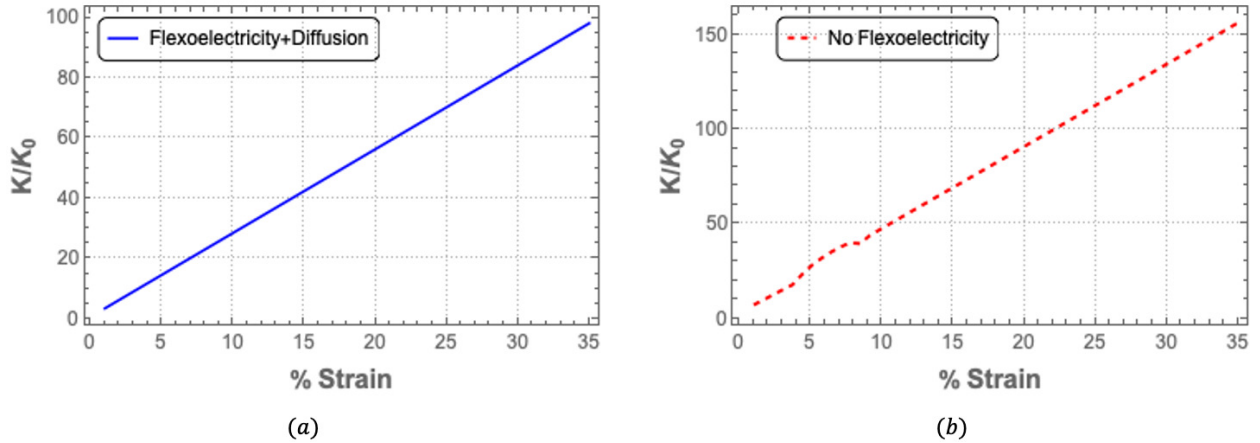


Figure 5: Normalized ionic conductivity of a thin film of thickness 100 nm as a function of uniaxial strain for 5(a) an electro-elastic-diffusive system with flexoelectricity, and 5(b) an electro-diffusive system without flexoelectricity.

The reason for this rather unexpected effect of flexoelectricity on ionic conductivity can be illustrated using Figure 6. It shows the polarization for a 50 nm PVDF thin film for the three different cases, namely, electro-elastic-diffusive system with flexoelectricity, electro-diffusive system without flexoelectricity, and flexoelectric system without diffusion. Since our boundary conditions dictate that the chemical potential at $x_1 = 0$ is higher than that at $x_1 = w$, ions flow from the bottom to the top of the film. Hence, as shown in Figure 6(b), the polarization due to the diffusion of ions is negative, that is, acting in the downward direction, opposite to the flow of ions. Moreover, it increases in magnitude from the top surface to the bottom surface. In contrast, Figure 6(c) shows that the net polarization due to flexoelectricity in the absence of diffusion of ions is zero. Nevertheless, Figure 6(a) reveals that under the combined effect of flexoelectricity and diffusion, polarization is negative and almost constant through the film thickness. This implies that the total polarization induced by flexoelectricity and diffusion is more complex than simply adding the polarization due to the two phenomena. Moreover, the polarization induced by flexoelectricity creates a resistance to the flow of ions which in turn reduces the ionic conductivity.

Figure 7 shows the results for displacement, chemical potential, and polarization obtained for a film thickness of 10 nm at 5% strain. The plots shown in Figure 7(a) for displacement and 7(d) for polarization due to flexoelectric effect without diffusion are consistent with the results for a thin film with flexoelectricity presented by Sharma et al. [45].

5. Conclusion

In this paper, we present a nonlinear continuum theory that integrates mechanical, electrical, and chemical coupled phenomena in flexoelectric-elastic-diffusive systems. By combining elements from existing literature on continuum mechanics of electro-elastic-diffusive systems and the theory of flexoelectricity, our study bridges the gap between these theories to present a nonlinear electro-chemo-mechanical theory incorporating flexoelectricity for soft materials. By applying this theoretical framework to a specific boundary problem of a thin film we gain insights into the effect of the coupling of flexoelectricity and diffusion on the ionic conductivity of thin films made of soft materials. The thin film example reveals that flexoelectricity can have a dramatic impact on ionic conductivity due to the interplay between the polarization induced by the flexoelectric effect and the flow of ions. Although our theoretical formulation is general, we chose a simple one-dimensional boundary value problem to demonstrate its application to soft solid electrolytes. The proposed theory can open avenues for further investigations into complex systems which would have real-world applications specifically in the field of energy harvesting or electromechanical phenomena in biological systems where flexoelectricity plays a vital role.

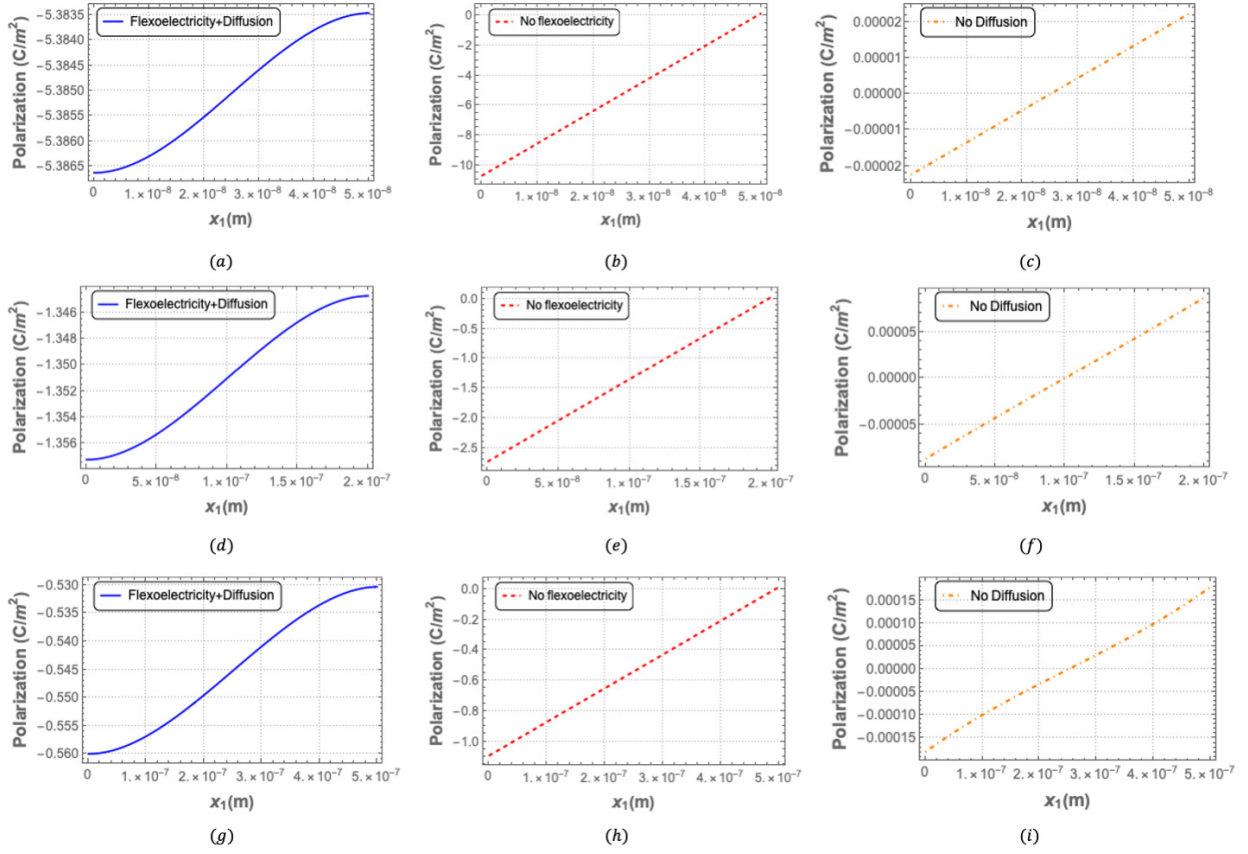


Figure 6: Variation of polarization along the thickness direction for a thin film for three systems– electro-elastic-diffusive system with flexoelectricity (blue), electro-diffusive system without flexoelectricity (red), and electromechanical system with flexoelectricity without diffusion (orange). Plots 6(a), 6(b) and 6(c) show polarization for a 50 nm thin sheet. Likewise, plots 6(d), 6(e) and 6(f) show polarization for a 200 nm thin sheet, while plots 6(g), 6(h) and 6(i) show polarization for a 500 nm thin sheet.

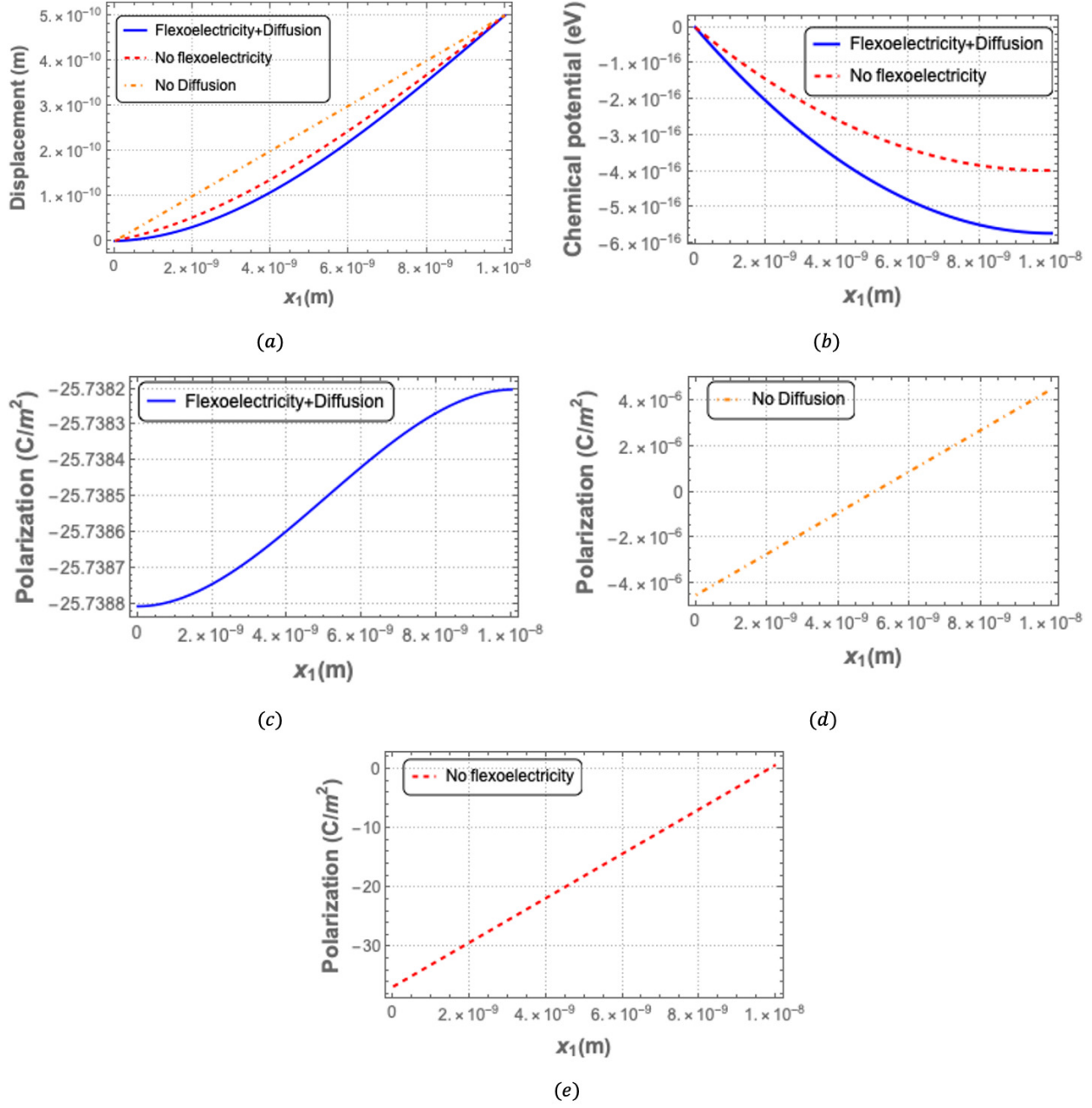


Figure 7: Displacement, polarization, and chemical potential plotted along the thickness direction for a 10 nm thin film for three cases – electro-elastic-diffusive system with flexoelectricity, electro-diffusive system without flexoelectricity, and flexoelectric system without diffusion. 7(a) compares the displacements for the three systems. 7(b) compares the chemical potential between electro-elastic-diffusive system with flexoelectricity and without. 7(c), 7(e), and 7(d) show the polarization along the thickness direction for the three systems respectively.

260 **Acknowledgment**

The authors thank Professor Pradeep Sharma, and Dr. Kosar Mozaffari for insightful discussions. The authors also gratefully acknowledge the support of NSF under grant DMR-2210155 and the Bill D. Cook Professorship.

Appendix A. Derivation of Ionic conductivity

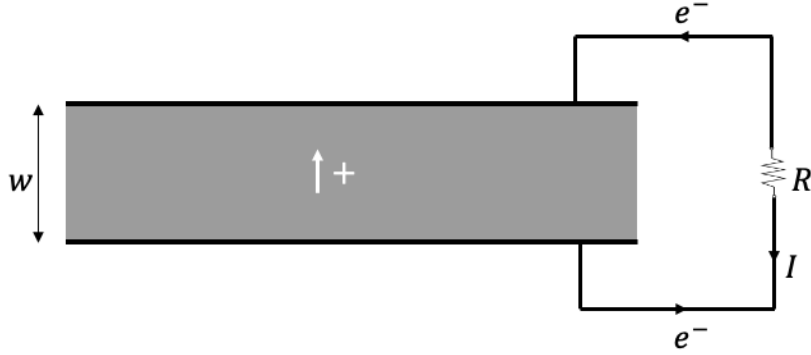


Figure A.8: Schematic of a single layer of electrolyte of width w . The direction of the flow of positive ions is shown by the white arrow.

265 Here, we summarize the approximate expression for ionic conductivity derived in Mozaffari et al [38]. As shown in Fig. A.8, let the single layer be subjected to the electrochemical potential, chemical potential, and electric potential denoted by $\nabla\phi$, $\nabla\mu$, and $\nabla\xi$ at the ends of the electrolyte respectively. Let the resistance in the external circuit be R . The total current in the external circuit is given by $I = \Delta\xi/R$. J is the ionic flux which is given by the expression $J = \frac{I}{qA}$. Here, A is the normal surface area of the contact electrode with the electrolyte. Ionic conductivity K satisfies the equation,

$$J = -K \frac{\nabla\phi}{w} \quad (\text{A.1})$$

From Eq. (53)₁ we get the following equation which gives a representation of K in terms of ionic concentration,

$$\nabla\phi = -\frac{Jw}{K} = -\int_0^w \frac{J}{\gamma c(x)} \quad (\text{A.2})$$

Substituting the above equation in Eq. (A.1) we get the expression for ionic conductivity,

$$K = \left[\frac{1}{w} \int_0^w \frac{J}{\gamma c(x)} dx \right]^{-1} \quad (\text{A.3})$$

Appendix B. Material properties for PVDF

275 The values are summarized in Table B.1. The expression $\frac{(bC-h^2)\epsilon_0}{C(1+a\epsilon_0)}$ has the same order as the radius of gyration (2.8×10^{-7} m). The value of the parameter b , thus is estimated using this relation as 9.927×10^{-3} N·m⁴/C². The order of e and f are the same as they occur only simultaneously in the governing equations. The initial concentration is taken as 50 mol and the chemical potential of pure ion is taken as 0.5 eV [38].

280 The flexoelectric coefficients and Young's modulus are taken from [28] and [46] respectively. Refer to [38] and [47] for the numerical values for diffusion-related material constants.

Serial No.	Parameter	Value and Units
1	b	$9.927 \times 10^{-3} \text{ N}\cdot\text{m}^4/\text{C}^2$
2	c	3.7 GPa
3	f	$-179 \text{ N}\cdot\text{m}/\text{C}$
4	a	$1.38 \times 10^{10} \text{ N}\cdot\text{m}^2/\text{C}^2$
5	ϵ_r	10
6	ϵ_0	$8.854 \times 10^{-12} \text{ C}^2/\text{N}\cdot\text{m}^2$
7	μ_0	0 eV
8	$\hat{\mu}$	0.5 eV
9	λ_r	$4 \times 10^{-9} \text{ m}$
10	α_{el}	$4 \times 10^{-9} \text{ J}$
11	β	$\sqrt{\frac{q^2 \lambda^2}{\epsilon_r \epsilon_0}} = 4.62 \times 10^{-46} \text{ N}^{1/2} \cdot \text{m}^2$
12	q	$1.6 \times 10^{-19} \text{ C}$
13	c_0	50 mol
14	γ	$1000 \text{ m}^2/\text{V}\cdot\text{s}$

Table B.1: Material properties of PVDF used in this example. Here, $\lambda_r (= \lambda\sqrt{\epsilon_r})$ is the Debye length for PVDF, γ is the mobility, c_0 is the initial concentration.

References

- [1] R. Zito and H. Ardebili, *Energy Storage: A New Approach*. Wiley-Scrivener, 2019.
- [2] M. R. Lukatskaya, B. Dunn, and Y. Gogotsi, "Multidimensional materials and device architectures for future hybrid energy storage," *Nature communications*, vol. 7, no. 1, p. 12647, 2016.
- 285 [3] S. Park, S. W. Heo, W. Lee, D. Inoue, Z. Jiang, K. Yu, H. Jinno, D. Hashizume, M. Sekino, T. Yokota, *et al.*, "Self-powered ultra-flexible electronics via nano-grating-patterned organic photovoltaics," *Nature*, vol. 561, no. 7724, pp. 516–521, 2018.
- [4] Y. Yang, "A mini-review: emerging all-solid-state energy storage electrode materials for flexible devices," *Nanoscale*, vol. 12, no. 6, pp. 3560–3573, 2020.
- 290 [5] C. V. Di Leo, E. Rejovitzky, and L. Anand, "A Cahn-Hilliard-type phase-field theory for species diffusion coupled with large elastic deformations: Application to phase-separating Li-ion electrode materials," *Journal of Mechanics Physics of Solids*, vol. 70, pp. 1–29, Oct. 2014.
- [6] V. A. Sethuraman, M. J. Chon, M. Shimshak, V. Srinivasan, and P. R. Guduru, "In situ measurements of stress evolution in silicon thin films during electrochemical lithiation and delithiation," *Journal of Power Sources*, vol. 195, pp. 5062–5066, aug 2010.
- 295 [7] A. Bower, P. Guduru, and V. Sethuraman, "A finite strain model of stress, diffusion, plastic flow, and electrochemical reactions in a lithium-ion half-cell," *Journal of the Mechanics and Physics of Solids*, vol. 59, no. 4, pp. 804–828, 2011.
- [8] F. Gao and W. Hong, "Phase-field model for the two-phase lithiation of silicon," *Journal of the Mechanics and Physics of Solids*, vol. 94, pp. 18–32, 2016.
- [9] M. Pharr, Z. Suo, and J. J. Vlassak, "Measurements of the fracture energy of lithiated silicon electrodes of li-ion batteries," *Nano Letters*, vol. 13, no. 11, pp. 5570–5577, 2013.
- 300 [10] J. Mendez, M. Ponga, and M. Ortiz, "Diffusive molecular dynamics simulations of lithiation of silicon nanopillars," *Journal of the Mechanics and Physics of Solids*, vol. 115, pp. 123–141, 2018.
- [11] S. Xu, Y. Zhang, J. Cho, J. Lee, X. Huang, L. Jia, J. A. Fan, Y. Su, J. Su, H. Zhang, *et al.*, "Stretchable batteries with self-similar serpentine interconnects and integrated wireless recharging systems," *Nature communications*, vol. 4, no. 1, p. 1543, 2013.
- 305 [12] M. Kammoun, S. Berg, and H. Ardebili, "Flexible thin-film battery based on graphene-oxide embedded in solid polymer electrolyte," *Nanoscale*, vol. 7, pp. 17516–17522, 2015.

- [13] M. Ganser, F. E. Hildebrand, M. Kamlah, and R. M. McMeeking, “A finite strain electro-chemo-mechanical theory for ion transport with application to binary solid electrolytes,” *Journal of the Mechanics and Physics of Solids*, vol. 125, pp. 681–713, 2019.
- [14] V. S. Deshpande and R. M. McMeeking, “Models for the Interplay of Mechanics, Electrochemistry, Thermodynamics, and Kinetics in Lithium-Ion Batteries,” *Applied Mechanics Reviews*, vol. 75, no. 1, p. 010801, 2023.
- [15] M. Winter and R. J. Brodd, “What are batteries, fuel cells, and supercapacitors?,” *Chemical reviews*, vol. 104, no. 10, pp. 4245–4270, 2004.
- [16] J. B. Goodenough and K.-S. Park, “The li-ion rechargeable battery: A perspective,” *Journal of the American Chemical Society*, vol. 135, no. 4, pp. 1167–1176, 2013.
- [17] H. Yang and N. Wu, “Ionic conductivity and ion transport mechanisms of solid-state lithium-ion battery electrolytes: A review,” *Energy Science & Engineering*, vol. 10, no. 5, pp. 1643–1671, 2022.
- [18] A. Manthiram, X. Yu, and S. Wang, “Lithium battery chemistries enabled by solid-state electrolytes,” *Nature Reviews Materials*, vol. 2, no. 4, pp. 1–16, 2017.
- [19] C. Li, Z.-y. Wang, Z.-j. He, Y.-j. Li, J. Mao, K.-h. Dai, C. Yan, and J.-c. Zheng, “An advance review of solid-state battery: Challenges, progress and prospects,” *Sustainable Materials and Technologies*, vol. 29, p. e00297, 2021.
- [20] Y. Koyama, T. E. Chin, U. Rhyner, R. K. Holman, S. R. Hall, and Y.-M. Chiang, “Harnessing the actuation potential of solid-state intercalation compounds,” *Advanced Functional Materials*, vol. 16, no. 4, pp. 492–498, 2006.
- [21] L. Liu, J. Xu, S. Wang, F. Wu, H. Li, and L. Chen, “Practical evaluation of energy densities for sulfide solid-state batteries,” *ETransportation*, vol. 1, p. 100010, 2019.
- [22] X. Rui, D. Ren, X. Liu, X. Wang, K. Wang, Y. Lu, L. Li, P. Wang, G. Zhu, Y. Mao, *et al.*, “Distinct thermal runaway mechanisms of sulfide-based all-solid-state batteries,” *Energy & Environmental Science*, vol. 16, no. 8, pp. 3552–3563, 2023.
- [23] K. Kezuka, T. Hatazawa, and K. Nakajima, “The status of sony li-ion polymer battery,” *Journal of power sources*, vol. 97, pp. 755–757, 2001.
- [24] Z. Yu, X. Zhang, C. Fu, H. Wang, M. Chen, G. Yin, H. Huo, and J. Wang, “Dendrites in solid-state batteries: Ion transport behavior, advanced characterization, and interface regulation,” *Advanced Energy Materials*, vol. 11, no. 18, p. 2003250, 2021.
- [25] H. Ardebili, “A Perspective on the Mechanics Issues in Soft Solid Electrolytes and the Development of Next-Generation Batteries,” *Journal of Applied Mechanics*, vol. 87, p. 040801, 11 2019.
- [26] S. Krichen and P. Sharma, “Flexoelectricity: A perspective on an unusual electromechanical coupling,” *Journal of Applied Mechanics*, vol. 83, no. 3, p. 030801, 2016.
- [27] Q. Deng, L. Liu, and P. Sharma, “Flexoelectricity in soft materials and biological membranes,” *Journal of the Mechanics and Physics of Solids*, vol. 62, pp. 209–227, 2014.
- [28] B. Chu and D. Salem, “Flexoelectricity in several thermoplastic and thermosetting polymers,” *Applied Physics Letters*, vol. 101, no. 10, 2012.
- [29] M. Grasinger, K. Mozaffari, and P. Sharma, “Flexoelectricity in soft elastomers and the molecular mechanisms underpinning the design and emergence of giant flexoelectricity,” *Proceedings of the National Academy of Sciences*, vol. 118, no. 21, p. e2102477118, 2021.
- [30] A. G. Petrov, “Flexoelectricity of model and living membranes,” *Biochimica et Biophysica Acta (BBA)-Biomembranes*, vol. 1561, no. 1, pp. 1–25, 2002.
- [31] A. Petrov, “Flexoelectricity of lyotropics and biomembranes,” *Il Nuovo Cimento D*, vol. 3, pp. 174–192, 1984.
- [32] L. P. Liu and P. Sharma, “Flexoelectricity and thermal fluctuations of lipid bilayer membranes: Renormalization of flexoelectric, dielectric, and elastic properties,” *Phys. Rev. E*, vol. 87, p. 032715, 2013.
- [33] P. Mohammadi, L. Liu, and P. Sharma, “A theory of flexoelectric membranes and effective properties of heterogeneous membranes,” *Journal of Applied Mechanics*, vol. 81, no. 1, p. 011007, 2014.
- [34] M. Torbati, K. Mozaffari, L. Liu, and P. Sharma, “Coupling of mechanical deformation and electromagnetic fields in biological cells,” *Rev. Mod. Phys.*, vol. 94, p. 025003, May 2022.
- [35] K. Mozaffari, F. Ahmadpoor, Q. Deng, and P. Sharma, “A minimal physics-based model for musical perception,” *Proceedings of the National Academy of Sciences*, vol. 120, no. 5, p. e2216146120, 2023.
- [36] A. Buka and N. Éber, *Flexoelectricity in liquid crystals: theory, experiments and applications*. World Scientific, 2013.
- [37] R. B. Meyer, “Piezoelectric effects in liquid crystals,” *Physical Review Letters*, vol. 22, no. 18, p. 918, 1969.
- [38] K. Mozaffari, L. Liu, and P. Sharma, “Theory of soft solid electrolytes: Overall properties of composite electrolytes, effect of deformation and microstructural design for enhanced ionic conductivity,” *Journal of the Mechanics and Physics of Solids*, vol. 158, p. 104621, 2022.
- [39] Q. Deng, L. Liu, and P. Sharma, “A continuum theory of flexoelectricity,” in *Flexoelectricity in Solids: From Theory to Applications*, pp. 111–167, World Scientific, 2017.
- [40] L. Anand, “A cahn–hilliard-type theory for species diffusion coupled with large elastic–plastic deformations,” *Journal of the Mechanics and Physics of Solids*, vol. 60, no. 12, pp. 1983–2002, 2012.
- [41] F. Darbaniyan, K. Dayal, L. Liu, and P. Sharma, “Designing soft pyroelectric and electrocaloric materials using electrets,” *Soft matter*, vol. 15, no. 2, pp. 262–277, 2019.
- [42] R. D. Mindlin, “Polarization gradient in elastic dielectrics,” *International Journal of Solids and Structures*, vol. 4, no. 6, pp. 637–642, 1968.
- [43] Q. Zheng and G.-W. Wei, “Poisson–boltzmann–nernst–planck model,” *The Journal of chemical physics*, vol. 134, no. 19, 2011.
- [44] W. R. Inc., “Mathematica, Version 13.3.” Champaign, IL, 2023.

- [45] N. Sharma, C. Landis, and P. Sharma, "Piezoelectric thin-film superlattices without using piezoelectric materials," *Journal of Applied Physics*, vol. 108, no. 2, 2010.
- 375 [46] H. Y. Guney, "Elastic properties and mechanical relaxation behaviors of pvdf (poly (vinylidene fluoride)) at temperatures between- 20 and 100° c and at 2 mhz ultrasonic frequency," *Journal of Polymer Science Part B: Polymer Physics*, vol. 43, no. 20, pp. 2862–2873, 2005.
- [47] Q. Deng, M. Kammoun, A. Erturk, and P. Sharma, "Nanoscale flexoelectric energy harvesting," *International Journal of Solids and Structures*, vol. 51, no. 18, pp. 3218–3225, 2014.